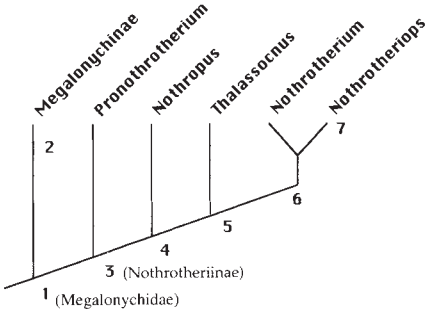

FIG. 4 Phylogenetic relationships of the Nothrotheriinae. The Nothrotheriinae are included within the Megalonychidae[27,28] in contrast to other interpretations, which relate them to the Megatheriidae[12,29]. Node 1, Megalonychidae: anterior tooth modified into caniniform and separated from cheek teeth by diastema, tuber calcis of calcaneum mediolaterally expanded, fifth metatarsal trapezoidal in shape with facets for cuboid and fourth metatarsal at oblique angle, third trochanter present on femur. Node 2, Megalonychinae: caniniform positioned at anterior margin of maxilla, cheek teeth triangular and bilophodont with transverse lophs convergent, medial trochlea of astragalus not modified into odontoid process, patellar surface of femur continuous with condylar surfaces. Node 3, Nothrotheriinae: caniniform positioned midway between anterior margin of maxilla and tooth row, cheek teeth quadrangular and bilophodont with transverse lophs parallel, longitudinal groove present on labial side of cheek teeth, post-palatine notch extends to last upper cheek tooth, supraorbital foramen present, predental spout of mandible elongated, ventral margin of predental spout straight, patellar groove of femur separated from condylar surfaces, astragalus with medial trochlea modified into odontoid process, proximal and second phalanges digit three pes co-ossified (unknown in *Nothropus*). Node 4, slight inflation of base of pterygoids. Node 5, loss of caniniform, post-palatine notch of palate positioned posterior to last upper cheek tooth, ventral margin of predental spout sigmoid relative to horizontal ramus, ungual phalanx of digit two of the manus dorsoventrally compressed. Node 6, pterygoids inflated with large pterygoid sinuses, ungual phalanx of digit one of the pes lost (unknown in *Thalassocnus*). Node 7, third trochanter forms continuous ridge with lateral epicondyle of femur.

The caudal vertebrae (Fig. 2*d–g*) of *Thalassocnus* have short but anteroposteriorly elongated transverse processes. In the first posterior caudal vertebrae, the transverse processes acquire a foramen for the passage of the segmental arteries[26]. In the more posterior caudals, the foramen opens laterally and the transverse process becomes bifurcated. This condition is absent in other sloths but is observed in otters (Fig. 2*h*) and beavers (Fig. 2*i*), semi-aquatic mammals capable of powerful dorsoventral strokes of the tail.

Thalassocnus therefore indicates another pathway by which a terrestrial group has shifted to an aquatic habitat. The anatomical features are different from those in other semi-aquatic mammals (hippos, desmostylians, aquatic rodents, aquatic carnivores) because of the inherent restriction due to the anatomical constraints of being a sloth. In fact there seems to be many ways in which a mammal can become aquatic or semi-aquatic.

Thalassocnus is a nothrotheriine megalonychid (Fig. 4) which was living on the beaches of the Pliocene desert coast of the southern Peru. We suggest that it had semi-aquatic habits and was entering the near-shore waters (femur and patella morphology) where it grazed on sea-grasses or seaweeds (premaxilla morphology). Strong dorsoventral movements of the tail (morphology of the caudal vertebrae) would have helped to maintain a head-down feeding position. Swimming could have been by paddling of the hind limbs (morphology of femur head and length of tibia). *Thalassocnus* was certainly not a fast swimmer, but the taphonomy strongly supports semi-aquatic habits and the anatomy is consistent with this interpretation. □

Received 1 February; accepted 22 March 1995.

1. Marshall, L. G. & Cifelli, R. L. *Palaeovertebrata* **19,** 169–210 (1990).
2. Webb, D. in *The Great American Biotic Interchange* (eds Stehli, G. & Webb, D.) 357–386 (Plenum, New York, 1985).
3. White, *J. J. vert Paleont.* **13,** 230–242 (1993).
4. Hoffstetter, R. *C. r. hebd. Séanc. Acad. Sci., Paris* D**267,** 1273–1276 (1968).
5. Muizon, C. de *Ed. Rech. gr. Civilisations, mém.* **6,** 1–150 (*Trav. Inst. Fr. Et. Andines* 22) (1981).
6. Muizon C. de & DeVries, T. J. *Geol. Rdsch.* **74,** 547–563 (1985).
7. Alpers, C. N. & Brimhall, C. H. *Geol. Soc. Am. Bull.* **100,** 1640–1651, (1988).
8. Sébrier, M., Marocco, R. & Macharé, J. in *Montagnes et Piedmonts* 49–69 (Revue Géographique des Pyrénées et du Sud-Ouest, Spec. issue, Toulouse, 1984).
9. Muizon, C. de & Bellon, H. *C. r. hebd. Séanc. Acad. Sci., Paris* D**290,** 1063–1066 (1981).
10. Muizon, C. de & Bellon, H. *C. r. hebd. Séanc. Acad. Sci., Paris* **303,** 1401–1404 (1986).
11. Cartelle, C. & Fonseca, J. S. *Lundiana* **2,** 127–181 (1983).
12. Paula Couto, C. *Tratado de Paleomastozoologia* (Acad. Bras. Ci., Rio de Janeiro, 1979).
13. Frailey, C. D. *Contr. Sci. Nat. Hist. Mus. L. A. Co.* **374,** 1–46 (1986).
14. Stock, C. *Publs Carnegie Instn* **331,** 1–206 (1925).
15. Muizon, C. de *Ed. Rech. Civilisations, mém.* **50,** 1–188 (*Trav. Inst. Fr. Et. Andines* 27) (1984).
16. Muizon, C. de *Ed. Rech. Civilisations mém.* **78,**, 1–244 (*Trav. Inst. Fr. Et. Andines* 42) (1988).
17. Muizon, C. de *Nature* **365,** 745–748 (1993).
18. Marocco, R. & Muizon, C. de *Bull. Inst. Fr. Et. Andines* **27,** 105–117 (1988).
19. Cartelle, C. & Bohorquez, G. A. *Iheringia* **11,** 9–14 (1986).
20. Solounias, N., Teaford, M. & Walker, A. *Paleobiology* **14,** 287–300 (1988).
21. Hansen, R. M. *Paleobiology* **4,** 302–319 (1978).
22. Naples, V. *Contr. Sci. Nat. Hist. Mus. L.A. Co.* **389,** 1–21 (1987).
23. Paula Couto, C. *Annls. Acad. brasil Cienc.* **43**(suppl.), 499–513 (1971).
24. Owen, R. *Description of the Skeleton of an Extinct Gigantic Sloth*, Mylodon robustus, *Owen, with Observations on the Osteology, Natural Affinities, and Probable Habits of the Megatheroid Quadrupeds in General* (R. & J. Taylor, London, 1842).
25. White, J. L. *J. vert. Paleont.* **13,** 230–242 (1993).
26. Miller, M. E., Christensen, G. C. & Evans, H. E. *Anatomy of the Dog* (Saunders, Philadelphia, 1964).
27. Hoffstetter, R. *Traité de Paléont.* **VI,** 522–636 (Masson, Paris, 1958).
28. Mones, A. *Cour. Forsch.-Inst. Senckenberg* **82,** 1–625 (1986).
29. Patterson, B., Segall, W., Turnbull, W. D. & Gaudin, T. J. *Fieldiana Geol.* **24,** 1–79 (1992).

ACKNOWLEDGEMENTS. The research was funded by the Institut Français d'Études Andines (Lima, Peru) and the Muséum national d'Histoire naturelle (Paris, France). We thank D. Frey (Staatliches Museum für Naturkunde, Karlsruhe, Germany), K. Seymour (Royal Ontario Museum, Toronto) and B. Senut (Muséum national d'Histoire naturelle, Paris) who kindly gave access to the specimens under their care. Valuable insights were provided by G. F. Engelmann and C. E. Ray. Photographs are by D. Serrette (CNRS, Muséum national d'Histoire naturelle, Paris).

Experimentally induced transitions in the dynamic behaviour of insect populations

R. F. Costantino*, J. M. Cushing†, Brian Dennis‡ & Robert A. Desharnais§

* Department of Zoology, University of Rhode Island, Kingston, Rhode Island 02881, USA
† Department of Mathematics, University of Arizona, Tucson, Arizona 85721, USA
‡ Department of Fish and Wildlife Resources, University of Idaho, Moscow, Idaho 83844, USA
§ Department of Biology, California State University, Los Angeles, California 90032, USA

SIMPLE nonlinear models can generate fixed points, periodic cycles and aperiodic oscillations in population abundance without any external environmental variation. Another familiar theoretical result is that shifts in demographic parameters (such as survival or fecundity) can move a population from one of these behaviours to another[1–4]. Unfortunately, empirical evidence to support these theoretical possibilities is scarce[5–15]. We report here a joint theoretical and experimental study to test the hypothesis that changes in demographic parameters cause predictable changes in the nature of population fluctuations. Specifically, we developed a simple

model describing population growth in the flour beetle *Tribolium*[16]. We then predicted, using standard mathematical techniques to analyse the model, that changes in adult mortality would produce substantial shifts in population dynamic behaviour. Finally, by experimentally manipulating the adult mortality rate we observed changes in the dynamics from stable fixed points to periodic cycles to aperiodic oscillations that corresponded to the transitions forecast by the mathematical model.

We modelled the relationship linking larval, pupal and adult numbers at time $t+1$ to the number of animals at time t in the flour beetle (see ref. 9). The model is a system of three difference equations:

$$\begin{aligned} L_{t+1} &= bA_t \exp(-c_{ca}A_t - c_{el}L_t) \\ P_{t+1} &= L_t(1-\mu_l) \\ A_{t+1} &= P_t \exp(-c_{pa}A_t) + A_t(1-\mu_a) \end{aligned} \quad (1)$$

Here, L_t is the number of feeding larvae, P_t is the number of non-feeding larvae, and pupae and callow adults, and A_t is the number of mature adults, at time t; the unit of time (2 weeks) is taken to be the feeding larval maturation interval, so that after one unit of time a larva either dies or survives and pupates. This unit of time is also the cumulative time spent as a non-feeding larva, pupa and callow adult. The quantity $b>0$ is the number of larval recruits per adult per unit of time in the absence of cannibalism. The fractions μ_l and μ_a are the larval and adult probabilities, respectively, of dying from causes other than cannibalism. The exponential nonlinearities account for the cannibalism of eggs by both larvae and adults and the cannibalism of pupae by adults. The fractions $\exp(-c_{ca}A_t)$ and $\exp(-c_{el}L_t)$ are the probabilities that an egg is not eaten in the presence of A_t adults and L_t larvae. The fraction $\exp(-c_{pa}A_t)$ is the survival probability of a pupa in the presence of A_t adults.

For fitting to time-series data, the model was converted to a stochastic model with noise added on a logarithmic scale:

$$\begin{aligned} L_{t+1} &= bA_t \exp(-c_{ea}A_t - c_{el}L_t + E_{1t}) \\ P_{t+1} &= L_t(1-\mu_l)\exp(E_{2t}) \\ A_{t+1} &= [P_t \exp(-c_{pa}A_t) + A_t(1-\mu_a)]\exp(E_{3t}) \end{aligned} \quad (2)$$

Here E_{1t}, E_{2t} and E_{3t} are random noise variables assumed to have a joint multivariate normal distribution with means of zero.

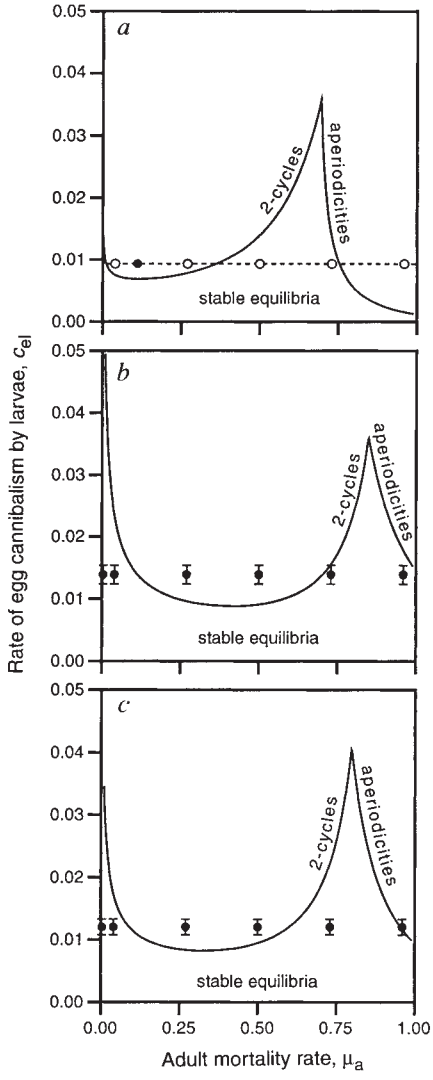

FIG. 1 Stability boundaries for the deterministic model (1) for three experiments. *a*, Sensitive strain[16] with $b=11.68$, $c_{ea}=0.011$, $c_{pa}=0.017$, $\mu_l=0.513$. The filled circle locates the population in parameter space. The broken line and open circles indicate the extrapolated predicted dynamic behaviour as a function of adult mortality. *b*, RR strain with $b=7.88$, $c_{ea}=0.011$, $c_{pa}=0.004$, $\mu_l=0.161$. *c*, SS strain with $b=7.48$, $c_{ea}=0.009$, $c_{pa}=0.004$, $\mu_l=0.267$. The filled circles locate the experimental populations in parameter space. In *b* and *c* the bar represents a 95% confidence interval for c_{el} based on the profile likelihood.

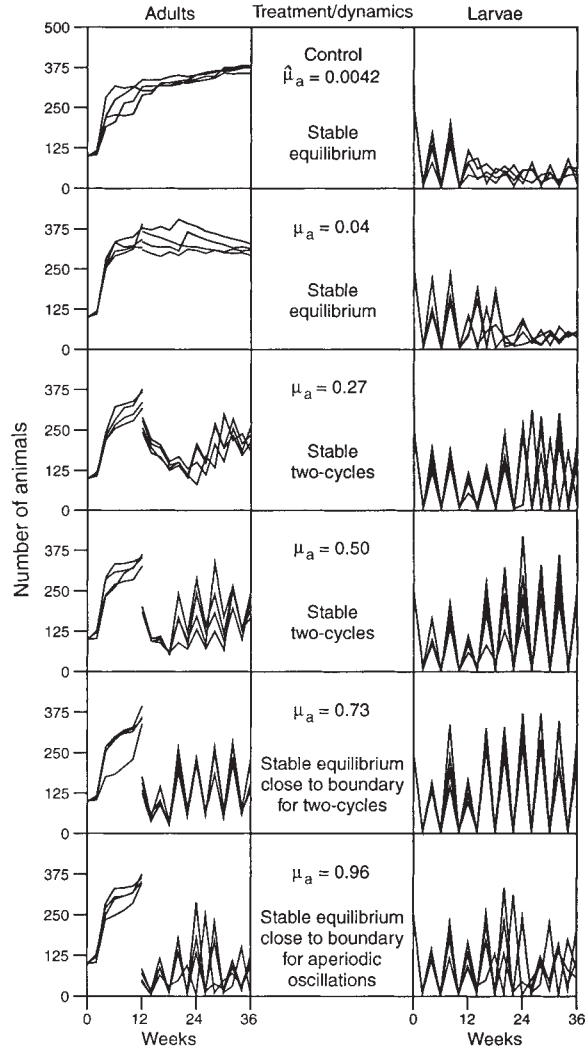

FIG. 2 Time-series data for individual replicates of the RR strain. At week 12 the experimental manipulation of adult mortality rate began. The centre column lists the imposed adult mortality rates and the location of the cultures in parameter space.

The noise variables represent the unpredictable departures of the observations from the deterministic model (1) due to environmental and other causes. Maximum-likelihood estimates of model parameters were calculated under the assumptions that the noise variables are correlated with each other but uncorrelated through time[16]. These assumptions were evaluated for all the data sets by standard diagnostic analyses of time-series residuals[17].

In the study reported here we experimentally set adult mortality rates at values suggested by the analysis of historical time-series data[16] (Fig. 1*a*) to place the experimental cultures in regions of different asymptotic dynamics: $\mu_a = 0.04$, 0.27, 0.50, 0.73 and 0.96. There were also control cultures which were not manipulated. Cultures of *T. castaneum* (24 for each of two genetic strains, RR and SS) were initiated with 100 young adults, 5 pupae and 250 small larvae. Each population was contained in a half-pint (237 ml) milk bottle with 20 g of standard media and kept in a dark incubator at 31 °C. Every two weeks the L_t, P_t, and A_t stages were censused and returned to fresh media. This procedure was continued for 36 weeks. At week 12, four populations of each genetic strain were randomly assigned to each of the six treatments, and the imposition of adult mortalities began. Adult mortality was manipulated by removing or adding adults at the time of a census to make the total number of adults that died during the interval consistent with the treatment value of μ_a. To counter the possibility of genetic changes in life-history characteristics, beginning at week 12 and continuing every month thereafter, the adults returned to the populations after the census were obtained from separate stock cultures maintained under standard laboratory conditions.

For each genetic strain the four replicates of each treatment were randomly assigned into two groups. With half of the data, we fitted model (2) to the time series of the RR (Fig. 2) and SS (Fig. 3) strains. The other half of the data were used for evaluating the model predictions. Analyses of time-series residuals[17] indicated that the stochastic model described the data quite well. Using the model and maximum-likelihood parameter estimates, based on the time series for weeks 12 to 36, we calculated the stability boundaries (Fig. 1*b*, *c*) and bifurcation diagrams (Fig. 4) for each genetic strain.

The parameter estimates placed the control and $\mu_a = 0.04$ treatments in the region of stable equilibria. In the $\mu_a = 0.27$ treatment there was a transition in the dynamics: regular, albeit small, fluctuations were found in the adult data, whereas large and sustained oscillations were noted in larval numbers. These populations were located in the two-cycle zone. At $\mu_a = 0.50$ both strains were in the two-cycle region and displayed sustained oscillations, most noticeably in larval numbers. With $\mu_a = 0.73$ the RR strain was close to the two-cycle boundary but the SS strain underwent another transition and was clearly in the region of stable equilibria. Fluctuations in the RR strain were sustained (Fig. 2) whereas the fluctuations in the SS strain appeared to dampen (Fig. 3).

In the $\mu_a = 0.96$ treatment both strains underwent another transition in the dynamics. The RR strain was in the stable equilibria region and the SS strain was in the region of aperiodic oscillations; however, both were close to the boundary at which a bifurcation to aperiodicities occurs (Fig. 1*b*, *c*). Being close to the aperiodic bifurcation boundary means that the transients of

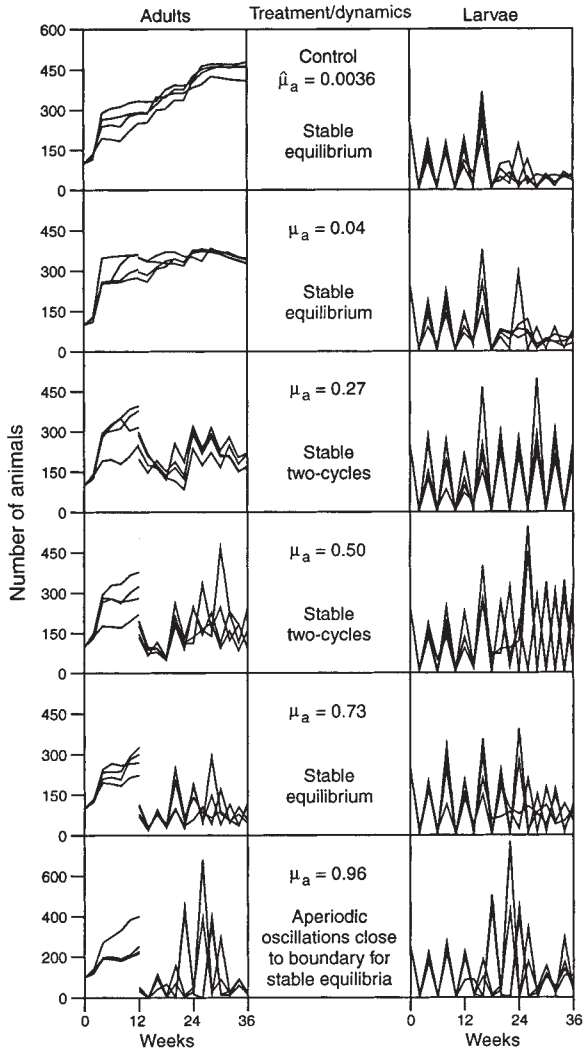

FIG. 3 Time-series data for individual replicates of the SS strain. At week 12 the experimental manipulation of adult mortality began. The centre column lists the imposed adult mortality rates and the location of the cultures in parameter space.

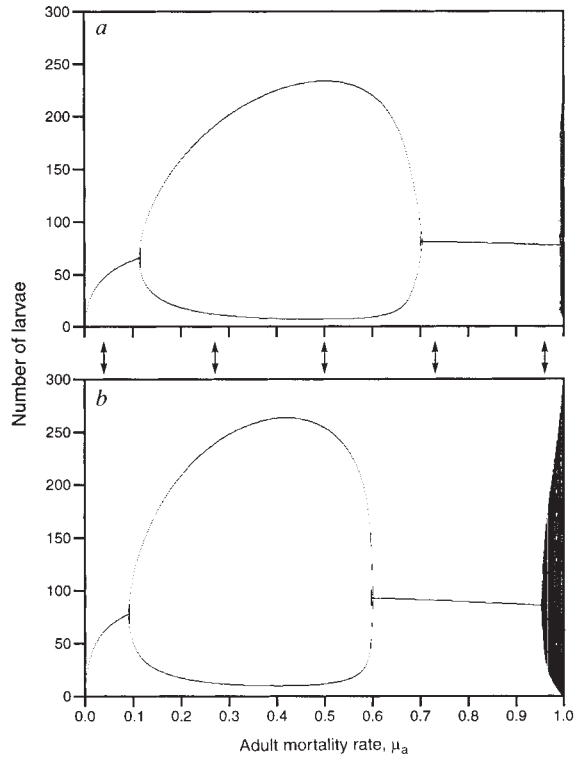

FIG. 4 Bifurcation diagrams for the model equations (1) for parameter values based on the experimental data. *a*, RR strain; *b*, SS strain. The double arrows indicate the adult mortality rate treatments.

the RR strain are expected to appear aperiodic and only slowly decay into the equilibrium. Both genetic strains displayed the expected aperiodic fluctuations (Figs 2 and 3).

Oscillatory approaches to point equilibria, stable periodic oscillations and aperiodic oscillations are difficult to distinguish in short time series with model-free methods. Our model-based parametric approach to classifying dynamic behaviour is statistically more powerful than non-parametric regression methods[18] or parametric flexible-response-surface methods[19]. However, our classifications depend on the adequacy of the model (2). We minimized the risk of error by basing the model on detailed knowledge of a well-studied system[9] and by thorough diagnostic analyses of the resulting time-series residuals[16]. The data (Figs 2 and 3) also give a visual impression of dynamic behaviours consistent with our classifications. Other, less-studied systems require statistical approaches that are more robust to variations in model form[20].

Our joint theoretical and experimental study has documented the transitions in the asymptotic dynamics of laboratory cultures of *Tribolium*. This rigorous verification of the predicted shifts in dynamical behaviour provides convincing evidence for the relevance of nonlinear mathematics in population biology. □

Received 21 December 1994; accepted 30 March 1995.

1. May, R. M. *Science* **186,** 645–647 (1974).
2. May, R. M. *J. theor. Biol.* **51,** 511–524 (1975).
3. May, R. M. *Nature* **261,** 459–467 (1976).
4. May, R. M. & Oster, G. F. *Am. Nat.* **110,** 573–599 (1976).
5. Strong, D. R. in *Ecological Theory and Integrated Pest Management* (ed. Kogan, M.) 37–58 (Wiley, New York, 1986).
6. Kareiva, P. in *Perspectives in Ecological Theory* (ed. Roughgarden, J., May, R. M. & Levin, S. A.) 68–88 (Princeton University Press, Princeton, NJ, 1989).
7. Bartlett, M. S. *J. R. statist. Soc.* A**52,** 321–347 (1990).
8. Logan, J. A. & Hain, F. (eds) *Chaos and Insect Ecology* (Virginia Polytechnic Institute and State University, Blacksburg, VA, 1991).
9. Costantino, R. F. & Desharnais, R. A. *Population Dynamics and the* Tribolium *Model: Genetics and Demography* (Springer, New York, 1991).
10. Logan, J. A. & Allen, J. C. *A. Rev. Ent.* **37,** 455–477 (1992).
11. Hastings, A., Hom, C. L., Ellner, S., Turchin, P. & Godfray, H. C. J. *A. Rev. Ecol. Syst.* **24,** 1–33 (1993).
12. Murdock, W. W. & McCauley, E. *Nature* **316,** 628–630 (1985).
13. Grenfell, B. J., Price, O. J., Albon, S. D. & Clutton-Brock, T. H. *Nature* **355,** 823–826 (1992).
14. Hanski, I., Turchin, P., Korplmäkl, E. & Henttonen, H. *Nature* **364,** 232–235 (1993).
15. Tilman, D. & Wedin, D. *Nature* **353,** 653–655 (1991).
16. Dennis, B., Desharnais, R. A., Cushing, J. M. & Costantino, R. F. *Ecol. Monogr.* (in the press).
17. Tong, H. *Non-linear Time Series: a Dynamical System Approach* (Oxford Univ. Press, Oxford, 1990).
18. McCaffrey, D. J., Ellner, S., Gallant, A. R. & Nychka, D. W. *J. Am. statist. Ass.* **87,** 682–695 (1992).
19. Turchin, P. & Taylor, A. *Ecology* **73,** 289–305 (1992).
20. Turchin, P. *Oikos* **68,** 167–172 (1993).

ACKNOWLEDGEMENTS. This work was supported by the NSF.

Interactions in the flexible orientation system of a migratory bird

Kenneth P. Able & Mary A. Able

Department of Biological Sciences, State University of New York, Albany, New York 12222, USA

MIGRATING **birds rely on interacting compass senses: magnetic, star, polarized light and perhaps Sun compasses[1,2]. During the development of orientation mechanisms, celestial rotation of stars at night[3] and of polarized skylight patterns during the day time[4] provide information about true compass directions that calibrates the direction of migration selected using the magnetic compass[3 11]. It might often be advantageous to adjust the magnetic preference by a geographic reference, especially at high northern latitudes where magnetic declination is large. Paradoxically, a magnetic preference so calibrated will be reliable only within a region of similar declination unless magnetic orientation remains open to calibration in older birds, something that earlier studies suggested was not the case[1,2]. We report here that in the Savannah sparrow (*Passerculus sandwichensis*) the same sort of calibration of magnetic orientation found in very young birds also occurs in older individuals exposed during the migration period to clear day and night skies within a shifted magnetic field.**

The Savannah sparrow is a medium-distance nocturnal migrant that nests in grassland, meadow and tundra across North America from the northern United States northwards to 60–70° N. It migrates to the southern United States southward to northern Central America in winter. Adult Savannah sparrows possess magnetic[12,13] and star compasses[8], and use visual cues associated with clear sunset skies (including skylight polarization patterns)[2,14,15] for orientation. We captured Savannah sparrows in local breeding fields in early September, 1994, before autumn migration. Of the 39 birds used in the experiment, 11 were adults (older than 1 year) and 28 were born during the 1994 nesting season (immature) (age determined by degree of skull ossification). Except during experimental and control treatments, the birds were housed in individual cages in a normal magnetic field and under ambient photoperiod, but had no exposure to the outdoors or sky. Groups of 10 birds were placed in a single cage centred within a large (2.7 m) Rubens coil[16] that was used to shift the magnetic field direction. The birds remained in the cage day and night until the group had experienced four clear days and four clear nights. They were then returned to individual cages and their magnetic orientation recorded in covered Emlen funnel orientation cages[17] during tests conducted indoors. Each group of birds was exposed to the day and night sky within coils under two conditions: (1) in an unshifted magnetic field (5.5×10^4 nT; inclination, 70°; declination, 13° W) (control condition); and (2) in a magnetic field (5.6×10^4 nT; inclination, 64°) shifted either 90° clockwise or 90° anticlockwise (shift condition). Orientation was recorded from each individual following each type of exposure (see Table 1 for details).

TABLE 1 Experimental treatments

	Group	Order of tests	Field shift	Dates of exposure (1994) C	S
(1)	4 adults, 6 immatures	C, S	90° CCW	9 Oct.–13 Oct.	18 Oct.–27 Oct.
(2)	3 adults, 6 immatures	S, C	90° CCW	27 Oct.–31 Oct.	13 Oct.–18 Oct.
(3)	4 adults, 6 immatures	C, S	90° CW	13 Oct.–18 Oct.	3 Nov.–15 Nov.
(4)	10 immatures	S, C	90° CW	15 Nov.–24 Nov.	27 Oct.–31 Oct.

C, Outdoor exposure in unshifted magnetic field (control condition); S, outdoor exposure in shifted magnetic field (shifted field condition); CCW, counterclockwise; CW, clockwise.

Savannah sparrows typically show axially bimodal magnetic migration orientation when tested over several nights[8,10,13]. Individual birds usually orient in a unimodal direction in each test, but often switch to more or less opposite directions on subsequent nights. This is true of hand-raised birds as well as wild-caught immatures and adults. Tested immediately after outdoor exposure in the control condition, both adults and immatures exhibited NNW–SSE magnetic orientation (Fig. 1*a*), typical of Savannah sparrows that have been raised outdoors in situations where magnetic and geographic directions were roughly coincident[4,8,10,13]. After exposure under the shifted field condi-